Supersonic Flutter Analysis Based on a Local Piston Theory

Wei-Wei Zhang,* Zheng-Yin Ye,† and Chen-An Zhang‡
Northwestern Polytechnical University 710072 Xi'an, People's Republic of China
and
Feng Liu§
University of California, Irvine, Irvine, California 92697-3975

A highly efficient local-piston theory is presented for the prediction of inviscid unsteady pressure loads at supersonic and hypersonic speeds. A steady mean flow solution is first obtained by an Euler method. The classical piston theory is modified to apply locally at each point on the airfoil surface on top of the local mean flow to obtain the unsteady pressure perturbations caused by the deviation of the airfoil surface from its mean location without the need of performing unsteady Euler computations. Results of two- and three-dimensional unsteady air loads and flutter predictions are compared with those obtained by the classical piston theory and an unsteady Euler method to assess the accuracy and validity range in airfoil thickness, flight Mach number, and angle of attack and with the presence of blunt leading edges. The local-piston theory is found to offer superior accuracy and much wider validity range compared with the classical piston theory, with the cost of only a fraction of the computational time needed by an unsteady Euler method.

Nomenclature

A	=	aerodynamic stiffness matrix
a	=	speed of sound
B	=	aerodynamic damping matrix
b	=	airfoil semichord
C_l	=	lift coefficient
C_m	=	moment coefficient
C_p	=	pressure coefficient
h	=	plunge displacement at the elastic axis, positive down
I_α	=	cross-sectional mass moment of inertia about its elastic axis
K_h, K_α	=	airfoil plunge stiffness, airfoil pitch stiffness
k	=	reduced frequency, $\omega_\alpha \cdot b/V_\infty$
M	=	Mach number
m	=	airfoil mass per unit span
p	=	pressure
r_α	=	dimensionless radius of gyration about elastic axis
S_α	=	static moment per unit span
t	=	physical time
x_α	=	dimensionless static imbalance of the airfoil about its elastic axis
V_f^*	=	reduced flutter speed
V_∞	=	freestream speed
α	=	angle of attack, torsion deflection
α_0	=	airfoil steady (mean) background flow angle of attack
$\delta\alpha$	=	amplitude of the pitch motion
μ	=	mass ratio, $m/\pi\rho b^2$
ρ	=	air density
τ	=	dimensionless time, $\omega_\alpha \cdot t$
ω	=	circular frequency, rad/s
ω_α, ω_h	=	uncoupled frequency of plunging and pitching

I. Introduction

WITH advances in computer technology and numerical algorithms, time-domain methods based on coupling the Euler or Navier–Stokes equations with structural dynamics equations have become a viable tool [1–4]. However, the major limitation of this method is the excessive cost of computational time and also the need of generating moving or deforming grids. Fast and accurate prediction of unsteady loads and flutter for air vehicles at high speeds remains to be a pressing engineering demand and an active research topic.

The piston theory [5–7] is an inviscid unsteady aerodynamic method that has been used extensively in supersonic and hypersonic aeroelasticity. Its ease of application and acceptable accuracy within its application range render the theory an effective tool for many aeroelastic problems, such as supersonic panel flutter analyses [8]. However, two inherent undesirable features of the classical piston theory invalidate its capability in general aeroelastic applications [9]. First, the theory is a strictly one-dimensional quasi-steady theory, whereby no upstream influence could be accounted for. Second, it is limited to thin wings at high Mach numbers and small angles of attack. The range of valid Mach numbers depends on the thickness and frequency parameters.

Linear-theory-based lifting-surface methods have been used for unsteady supersonic flow problems, such as ZONA51 code [10]. Nevertheless, these methods are confined to planforms of very thin sections at small angles of attack, whereby neither thickness effect nor angles of attack can be accounted for. A unified hypersonic-supersonic lifting-surface method (ZONA51U code [9]) has been developed in which the concept of the piston theory is generalized and suitably integrated with the aerodynamic influence coefficient matrix due to linear theory. This unified method can account for the effects of wing thickness and/or flow incidence, upstream influence, and three-dimensionality for an arbitrary lifting-surface system in an unsteady flow.

In this paper, a computational fluid dynamics (CFD)-based local piston theory method is developed and used for supersonic and

*Associate Professor, National Key Laboratory of Aerodynamic Design and Research. Member AIAA.
†Professor, National Key Laboratory of Aerodynamic Design and Research. Member AIAA.
‡Graduate Student, National Key Laboratory of Aerodynamic Design and Research.
§Professor, Department of Mechanical and Aerospace Engineering. Associate Fellow AIAA.

hypersonic flutter predictions. A steady flow solution is first obtained by an Euler method on any geometry. The piston theory is then applied locally at each point on the wing surface on top of the mean steady flowfield to obtain the unsteady pressure perturbations caused by the deviation of the surface from its mean location. Only one steady-state CFD solution is required for a flutter prediction at any one given flight condition. No time-domain unsteady computations and moving grids are needed. On the other hand, because the piston theory is applied locally, it greatly reduces the limitations of the classical piston theory on the flight Mach number, the shape of the airfoil, and the angle of attack.

II. Local Piston Theory

The classical piston theory can be found in a number of references [5–7]. Here, we will simply state its basic assumptions and final formulas. The piston theory assumes that disturbances spread along the normal to the surface for $M \gg 1$, as if caused by the action of a piston. From the use of the momentum equation and the assumption of isentropic perturbations, one obtains the following basic piston theory formula for the surface pressure:

$$p = p_\infty \left(1 + \frac{\gamma - 1}{2} \frac{W}{a}\right)^{\frac{2\gamma}{\gamma - 1}} \tag{1}$$

where W is the downwash speed, a is the sound speed of the free-stream, and γ is the radio of the specific heats. Therefore, the surface pressure coefficient becomes

$$C_p = \frac{2}{\gamma M^2} \left\{ \left(1 + \frac{\gamma - 1}{2} M \frac{W}{a}\right)^{\frac{2\gamma}{\gamma - 1}} - 1 \right\} \tag{2}$$

which we will call the full classical piston theory. For small perturbations ($M(W/a) \ll 1$), however, we may use the linearized first-order formula

$$C_p = \frac{2}{M^2} \left(\frac{W}{a}\right) \tag{3}$$

or the second-order formula:

$$C_p = \frac{2}{M^2} \left[\frac{W}{a} + \frac{\gamma + 1}{4} \left(\frac{W}{a}\right)^2\right] \tag{4}$$

In all of the preceding formulations, it is assumed that the pistonlike perturbation W is relative to the freestream conditions. As such, it must be limited to small perturbations, even though it contains both the disturbances by the mean position of the body and the unsteady fluctuations of the surface around its mean position. The latter can be assumed to be small for typical flutter applications, whereas the former may not unless we are limited to thin bodies and small angles of attack. To remove the limitations on the mean position of the body, we can separate the steady mean flow from the small unsteady fluctuations. This can be accomplished by solving the steady Euler equations for the full geometry. At each grid point on the surface, we may then apply the preceding piston theory relative to the local flowfield with the downwash caused by the deviation of the moving surface relative to its mean location. Figure 1 shows the decomposition of the local downwash velocity due to the motion of the

surface V_b. By applying Eq. (1) locally and keeping only the first-order terms, we obtain the following local piston theory:

$$\begin{cases} P = P_l + \rho_l a_l W \\ W = \mathbf{V}_l \cdot \delta\mathbf{n} + \mathbf{V}_b \cdot \mathbf{n} \\ \delta\mathbf{n} = \mathbf{n}_0 - \mathbf{n} \end{cases} \tag{5}$$

where $\boldsymbol{n}_0$ is the outward normal unit vector before deformation; $\boldsymbol{n}$ is the outward normal unit vector after deformation; W is the local downwash speed due to both deformation $\mathbf{V}_l \cdot \delta\boldsymbol{n}$ and vibration $\mathbf{V}_b \cdot \boldsymbol{n}$; P_l, ρ_l, a_l, and V_l are the local pressure, density, sound speed and flow velocity, respectively, on the mean wing surface computed by the full three-dimensional steady Euler method.

Compared with the classical piston theory, the preceding local piston theory accounts for three-dimensional effects and upstream influence through the use of the local mean flow. Because the local unsteady deviations are indeed small, the accuracy of the piston theory as applied locally is guaranteed, provided the local Mach number is not too low. In addition, even if the mean flow may not be isentropic because of the existence of shock waves, the unsteady perturbations locally at each grid point on the wing surface caused by the small deviations from its mean location may be regarded as isentropic. In terms of computational effort, only one steady-state solution is needed for each flight condition. The local piston theory yields an explicit algebraic point-function relationship, which is almost zero-cost computationally, between the unsteady pressure perturbations and the local airfoil motion or deformation. Therefore, the local piston theory greatly extends the range of applicability and accuracy of the classical piston theory at the cost of only one steady Euler solution for calculating unsteady aerodynamic loads at supersonic or hypersonic conditions.

III. Computation of Unsteady Aerodynamic Loads

To assess the validity and accuracy of the preceding local piston theory, we apply it to compute the unsteady pressure distributions and aerodynamic loads of some typical supersonic airfoils and compare the results with those by the classical piston theory and a full unsteady Euler code. Validation of the Euler code with experiments for steady and unsteady flow was documented in [11,12].

We first consider a symmetric circular-arc airfoil pitching around its quarter-chord position. The motion of the airfoil is described by $\alpha = \alpha_0 + \delta\alpha \cdot \sin(\omega \cdot t)$, where α_0 is the mean angle of attack, $\delta\alpha$ is the amplitude of the pitching motion, and ω is the frequency. The base airfoil has a thickness of 4% chord. The base flow conditions are chosen to be flight Mach number $M = 5$, mean angle of attack $\alpha_0 = 0$, pitching amplitude $\delta\alpha = 1$ deg, and a reduced frequency $k = (\omega b/V) = 0.1$. The classical piston theory is limited to only thin airfoils with sharp leading edges, small mean angle of attack, and limited Mach number range. In the following subsection, we vary the airfoil thickness, mean angle of attack, and flight Mach number to assess the expanded application range and enhanced accuracy of the local piston theory. We also investigate the applicability of the local piston method to an airfoil with a round leading edge (the NACA0012 airfoil). The time histories of the aerodynamic coefficients (including C_l, C_m and C_p) and the first mode of their Fourier expansions are compared with results of the full classical piston theory given by Eq. (2) and the full unsteady Euler computations for the various test cases. The unsteady Euler solutions are used as the benchmark solutions.

A. Effect of Airfoil Thickness

Figure 2 compares the first harmonic of the time-dependent lift and moment coefficients computed by the three methods for the airfoil thicknesses ranging from 4 to 16%. The phase of the lift coefficients by all three methods agrees well with each other for the complete thickness range. The amplitude of the two approximate methods, however, starts to deviate from that by the full unsteady Euler computations at thicknesses above 8%. The local piston theory agrees more
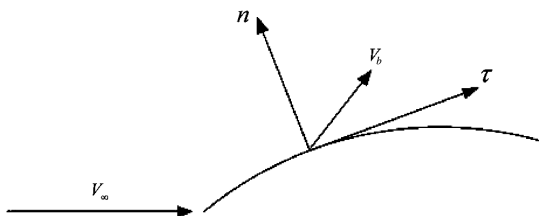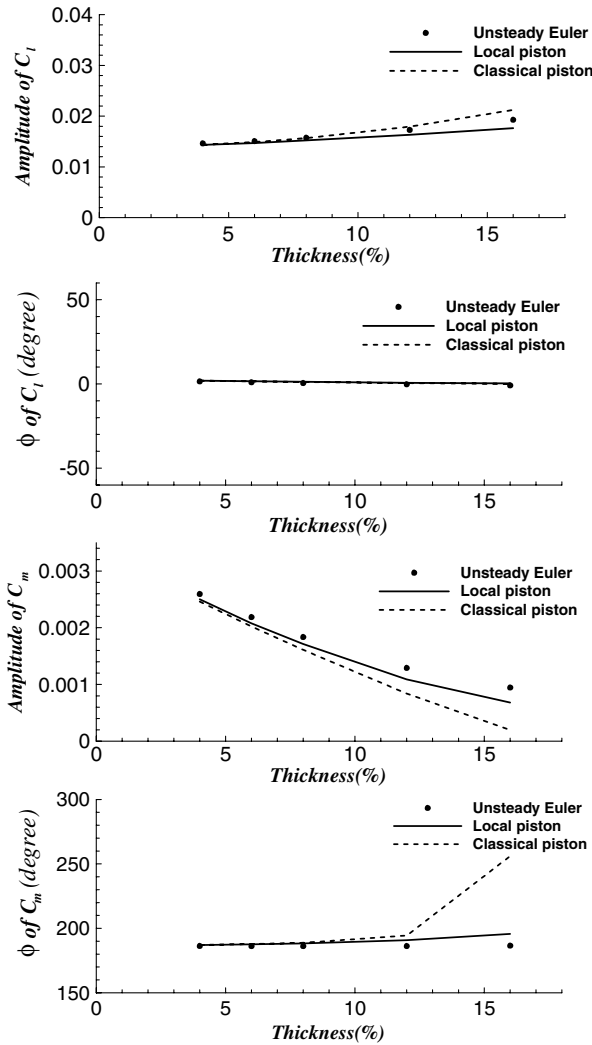

Fig. 1 Local velocity decomposition.

Fig. 2 Amplitude and phase of the first harmonic of C_l and C_m vs thickness of the circular-arc airfoil, $M = 5$ and $\alpha_0 = 0$.

Fig. 3 Time histories of C_l and C_m for the 12% thickness circular-arc airfoil, $M = 5$ and $\alpha_0 = 0$.

Fig. 4 Amplitude and phase of first harmonic of C_p for the 12% thickness circular-arc airfoil, $M = 5$ and $\alpha_0 = 0$.

closely with the Euler predictions for the larger thickness values. The advantages of the local piston theory are clearly seen in the moment coefficients. Both the amplitude and phase of the moment coefficient computed by the classical piston theory start to show large errors compared with the full unsteady Euler results for thicknesses above 8% and the errors become unacceptably large and diverge quickly as the thickness increases beyond 12%. The local piston theory, however, shows consistently better accuracy for the complete range of thicknesses. The errors are all within acceptable limit and do not diverge. Figure 3 shows the time histories of C_l and C_m for the 12% thickness airfoil. The errors in C_m by the classical piston theory are obvious, whereas those by the local piston theory are much smaller. Figure 4 compares the first harmonics of the unsteady pressure distribution on the same airfoil. The large error of the classical piston theory appears to be near the leading edge, which explains the large error in the moment coefficient. The local piston theory predictions closely follow those by the unsteady Euler code even for this large airfoil thickness.

B. Effect of Angle of Attack

Figure 5 shows the first harmonic of C_l and C_m at different mean angles of attack for the base 4% thickness airfoil. Other flow conditions are fixed and the same as the base conditions. The classical piston theory incurs monotonically increasing errors in the amplitude of both the lift and moment coefficients as the mean angle of attack increases and the errors become very large when the mean angle of attack is greater than 10 deg. The local piston theory,
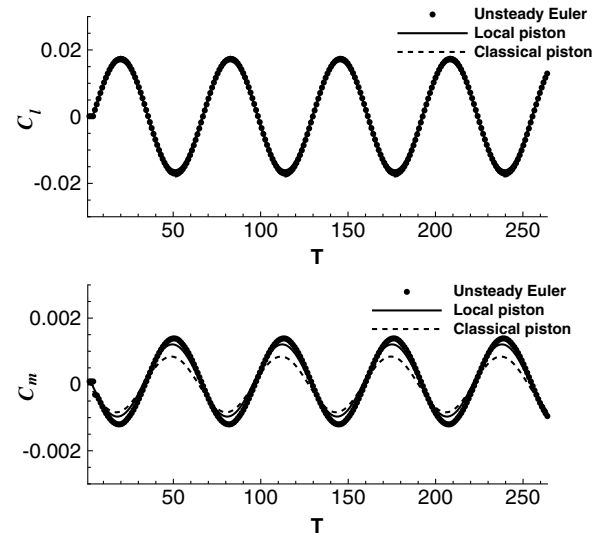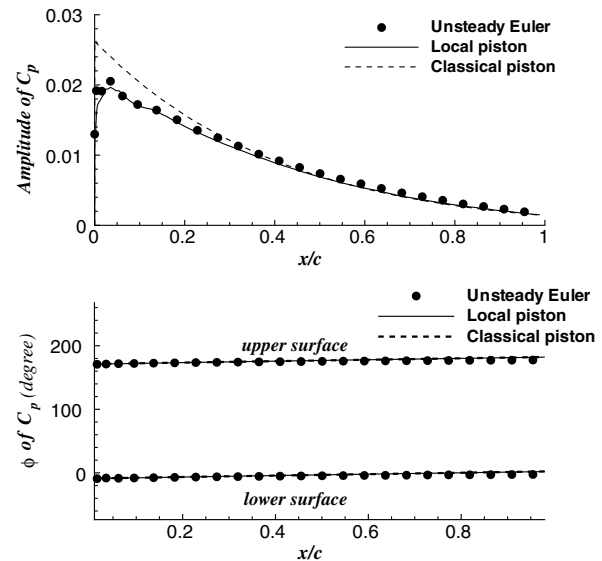
however, maintains high accuracy even for angles of attack up to 20 deg. The errors in the moment coefficient are a little more than those in the lift coefficient at the very large angles of attack, but remain still small. Figure 6 shows the time history of C_l and C_m for $\alpha_0 = 15$ deg, which corroborate on the same conclusions. Additionally, it shows that the mean level of the unsteady lift coefficient predicted by the classical piston theory is off significantly from the unsteady Euler solutions because of its approximate nature in predicting both the mean flow and the unsteady fluctuations at high angles of attack. The local piston theory eliminates this error in the mean flow through the use of local mean flow conditions that are accurately predicted by the steady Euler code. Figure 7 shows the first harmonics of the pressure coefficient distribution on the airfoil. As in the thickness studies, the local piston theory shows superior performance over the classical piston theory, which predicts an erroneous unsteady pressure amplitude on the pressure surface of the airfoil because of the existence of a strong shock from the leading edge of the airfoil at the 15 deg high mean angle of attack. The classical piston theory calculates the unsteady pressure perturbations from the freestream flow upstream of the shock rather than using the local flow conditions behind the shock.
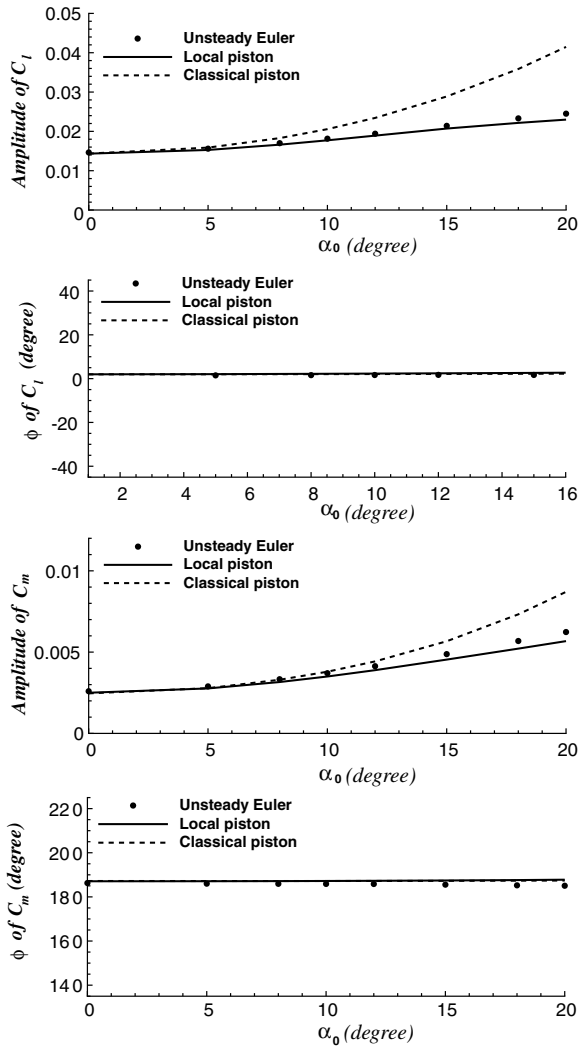
Fig. 5 Amplitude and phase of first-order harmonic of C_l and C_m vs mean angle of attack for the 4% circular-arc airfoil at $M = 5$.
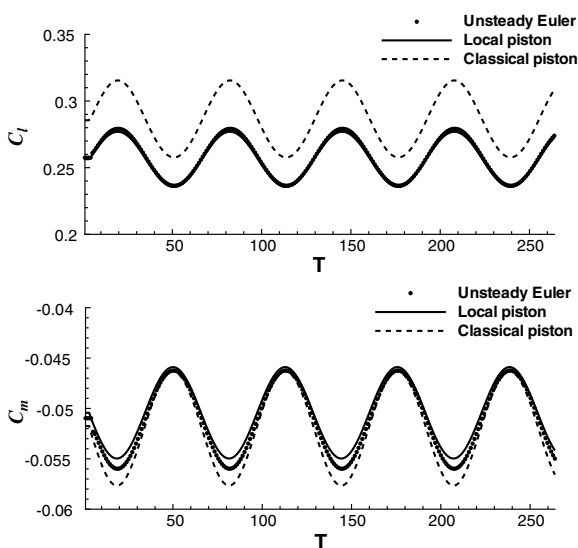

Fig. 6 Time histories of C_l and C_m for the 4% circular-arc airfoil at $M = 5$ and $\alpha_0 = 15\,\mathrm{deg}$.

C. Effect of Freestream Mach Number

The same preceding 4% base circular-arc airfoil test case is studied. Figure 8 compares the amplitude and phase of the first harmonic of the computed C_l and C_m at flight Mach numbers from
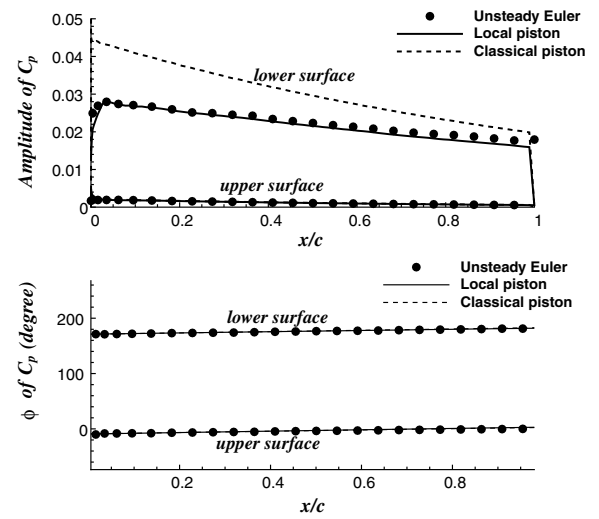

Fig. 7 Amplitude and phase of the first harmonic of C_p for the 4% circular-arc airfoil at $M = 5$ and $\alpha_0 = 15\,\mathrm{deg}$.
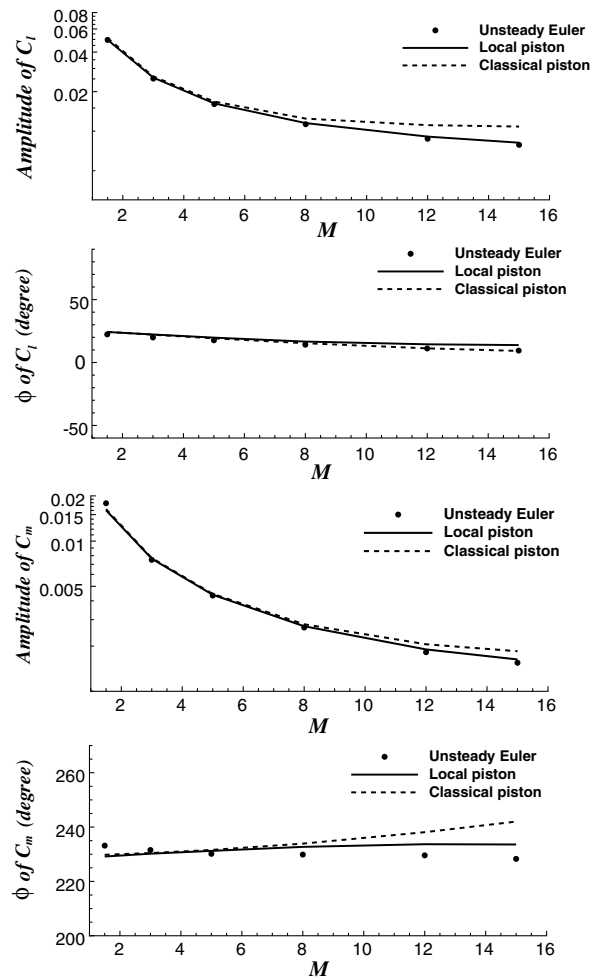

Fig. 8 Amplitude and phase of first harmonics of C_l and C_m vs flight Mach number for the 4% circular-arc airfoil.

1.5 to 15. This time, however, the flow conditions are chosen to be $\alpha_0 = 5\,\mathrm{deg}$, $\delta\alpha = 1\,\mathrm{deg}$, and $k = 1$. The classical piston theory deteriorates as the Mach number increases, except for the phase of C_l. The local piston theory maintains reasonably high accuracy even for Mach numbers up to 16. The typical unsteady pressure distributions on the airfoil is illustrated by those at $M = 12$, as shown in Fig. 9. The large discrepancy of the pressure amplitude on the pressure surface
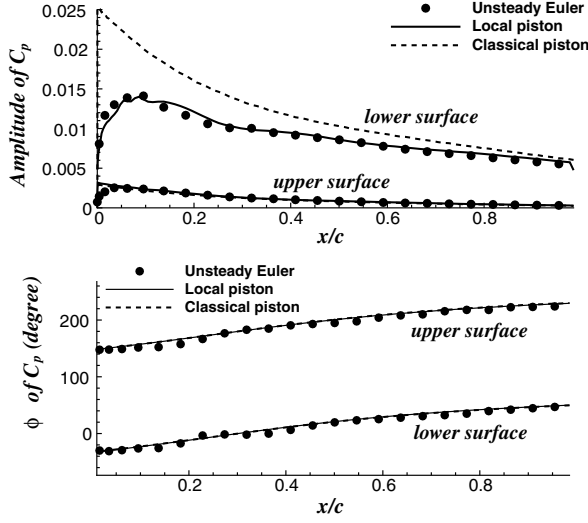
Fig. 9   Amplitude and phase of the first harmonic of C_p on the 4% circular-arc airfoil at $M = 12$.

Fig. 11   Amplitude and phase of the first harmonic of C_p for NACA0012 airfoil.

by the classical piston theory is due to the nonzero mean angle of attack, as discussed earlier, and made worse by the high Mach number. The local piston theory improves the accuracy on both fronts.

D.   Effect of Leading-Edge Shape

The classical piston theory is limited to airfoils with sharp leading edges. It fails when the slope of the airfoil approaches infinity at the round leading edge of a blunt airfoil. The NACA0012 airfoil is here used to demonstrate the feasibility of applying the local piston theory method to an airfoil with a round leading edge. We study the NACA0012 airfoil at $M = 8$, $k = 0.1$, $\alpha_0 = 0$ deg, and $\delta\alpha = 1$ deg. Figure 10 shows the time histories of the computed C_l and C_m for this case. Unacceptably large errors in both C_l and C_m are found in the classical piston theory. The local piston theory, on the other hand, gives surprisingly good predictions, especially for C_m. Figure 11 shows the first harmonic of the unsteady pressure on the airfoil. The local piston theory removes the singularity present in the classical piston theory, because it calculates the unsteady pressure loads by perturbing from the local flow conditions that have been correctly calculated by the steady Euler code, which takes care of the full thickness and rounded leading-edge shape without presenting any false singularities. The strict validity of the piston theory in a
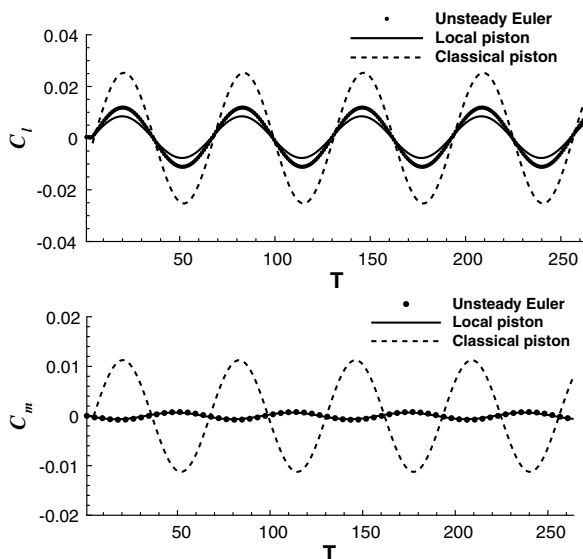
subsonic region is questionable even when it is applied locally. It may be fortuitous here that reasonably good results are obtained, but two factors are worth noting. First, the subsonic region is small and enclosed. Second, the major failure of the classical piston theory here is because of the spurious singularity at the leading edge.

IV.   Flutter Computations

The preceding section demonstrates that the local piston theory greatly improves the accuracy and extends the range of applicability of the classical piston theory for calculating supersonic and hypersonic unsteady aerodynamic loads. Large disturbances and nonlinearity caused by thickness, mean angle of attack, flight Mach number, and blunt leading edges are accounted by the steady Euler computation. Its computational efficiency lends it to use for fast flutter simulations and predictions. We consider the following modal equation as the general structural model:

$$\mathbf{M} \cdot \ddot{\boldsymbol{\xi}} + \mathbf{G} \cdot \dot{\boldsymbol{\xi}} + \mathbf{K} \cdot \boldsymbol{\xi} = \mathbf{F} \qquad (6)$$

where $\boldsymbol{\xi}$ is the generalized coordinate; $\mathbf{M}$, $\mathbf{G}$, and $\mathbf{K}$, are the mass, damping, and stiffness matrices, respectively; and $\mathbf{F}$ is the generalized aerodynamic force vector, for which the components are

$$F_i = \iint_s p(x, y, z, t)\boldsymbol{\Phi}_i(x, y, z)\,\mathrm{d}s$$

$$= q \cdot \iint_s C_p(x, y, z, t)\boldsymbol{\Phi}_i(x, y, z)\,\mathrm{d}s$$

where $\boldsymbol{\Phi}_i$ is the ith mode shape. A coupled fluid–structure simulation algorithm [13] can be used to integrate Eq. (6) in the time-domain along with any unsteady flow solver to determine the characteristics of the coupled aeroelastic system. Several such time-domain simulations are needed to determine the flutter boundary for each flight condition. Validation of the time-domain simulation method with the unsteady Euler flow solver for flutter predictions was documented in [12–14]. We can adopt the same coupled time-domain simulation method with either the classical or the local piston theory as the flow solver, both of which are far more efficient computationally because they involve only algebraic equations to determine the unsteady air loads.

With the local piston theory, however, an even more efficient alternative method can be used without having to perform such time-domain coupled simulations. Because of the linear algebraic dependence as given in Eq. (5) of the unsteady pressure $(p-p_l)$ on the local downwash velocity W, which in turn can be expressed as explicit linear functions of the local wing geometry and its moving velocity, one can obtain the following explicit expression for the generalized aerodynamic force $\mathbf{F}$:

Fig. 10   Time histories for the NACA0012 airfoil.

$$F = \frac{\rho V^2}{M} A \cdot \xi + \frac{\rho V}{M} B \cdot \dot{\xi} \qquad (7)$$

where A and B are the aerodynamic stiffness and damping matrices, respectively, the particular forms of which depend on the wing geometry and the mode shapes. Detailed formulas can be found in [12]. Substituting Eq. (7) into Eq. (6), we then obtain the following flutter equation:

$$[\dot{\xi}, \ddot{\xi}]^T = C \cdot [\xi, \dot{\xi}]^T \qquad (8)$$

where

$$C = \begin{pmatrix} 0 & I \\ M^{-1}\left(\frac{\rho V^2}{M} A \text{-} K\right) & \frac{\rho V}{M} M^{-1} B \end{pmatrix}$$

The flutter boundary can then be easily determined by computing the eigenvalue root loci of the matrix C vs V or ρ with little computational effort. Both this method and the time-domain coupled simulation method with the local piston theory as the flow solver have been performed for a number of test cases and found to give identical results. Because of its computational efficiency, results presented in this paper for the local piston theory are obtained by the eigenvalue analysis, which is several orders of magnitude more efficient than the time-domain unsteady Euler method, because it requires only one steady-state Euler computation for each flight condition.

In the following two subsections, we investigate application of the local piston theory to airfoil and wing flutter problems and compare the results with those by the classical piston theory and the full unsteady Euler computations.

A. Airfoil Test Cases

The following standard pitching and plunging model is used for two-dimensional airfoils:

$$\begin{cases} m\ddot{h} + S_\alpha \ddot{\alpha} + K_h h = -L \\ S_\alpha \ddot{h} + I_\alpha \ddot{\alpha} + K_\alpha \alpha = M \end{cases} \qquad (9)$$

In the form of Eq. (6), after defining the dimensionless time $\tau = \omega_\alpha \cdot t$ and the generalized coordinates

$$\xi = \begin{Bmatrix} h/b \\ \alpha \end{Bmatrix}$$

we obtain

$$M = \begin{bmatrix} 1 & x_\alpha \\ x_\alpha & r_\alpha^2 \end{bmatrix}, \qquad G = 0, \qquad K = \begin{bmatrix} (\omega_h/\omega_\alpha)^2 & 0 \\ 0 & r_\alpha^2 \end{bmatrix}$$

$$F = \frac{1}{\pi k^2 \mu} \begin{Bmatrix} -C_l \\ 2C_m \end{Bmatrix} = \frac{1}{\pi} \cdot V_f^{*2} \begin{Bmatrix} -C_l \\ 2C_m \end{Bmatrix}$$

where $k = \omega_\alpha \cdot b/V_\infty$, $\mu = m/\pi\rho b^2$, and $V_f^* = V_\infty/(\omega_\alpha \cdot b \cdot \mu^{1/2})$ are the reduced frequency, mass ratio, and the dimensionless speed index, respectively. The following structural parameters are used in the computations: $a = 0$, $x_\alpha = 0.25$, $r_\alpha^2 = 0.75$, $\omega_h/\omega_\alpha = 0.5$, and $\mu = 75$.

Two representative airfoils are considered: the 4% thickness circular-arc airfoil with a sharp leading edge and the NACA64A010 airfoil with a round leading edge. Figure 12 compares the computed flutter speed of the circular-arc airfoil for different flight Mach numbers at a 5 deg fixed angle of attack. The first-order, second-order, and precise piston theories labeled in the figure refer to the three levels of approximation of the classical piston theory given by Eqs. (2–4), respectively. As the Mach number increases, all three forms of classical piston theory incur an increasing amount of error. The accuracies of the three forms are in line with their corresponding order of the Taylor expansions, with the precise piston theory of Eq. (2) being the best. The local piston theory, however, gives consistently better predictions for the whole range of Mach numbers up to 10, with little error compared with the full unsteady Euler
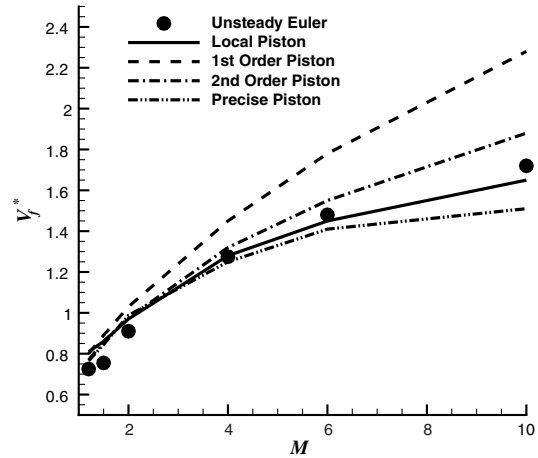

Fig. 12 Flutter speed vs Mach number for the circular-arc airfoil at a 5 deg angle of attack.

simulations. Figure 13 plots the flutter boundary of the same airfoil at the fixed flight Mach number $M = 6$, but for different angles of attack. The same observations can be made. This time, the local piston theory predictions almost exactly match those by the full unsteady Euler simulations. Considering the high accuracies of the local piston theory in predicting the unsteady air loads as presented in the last section, this level good agreement in flutter predictions is not surprising.
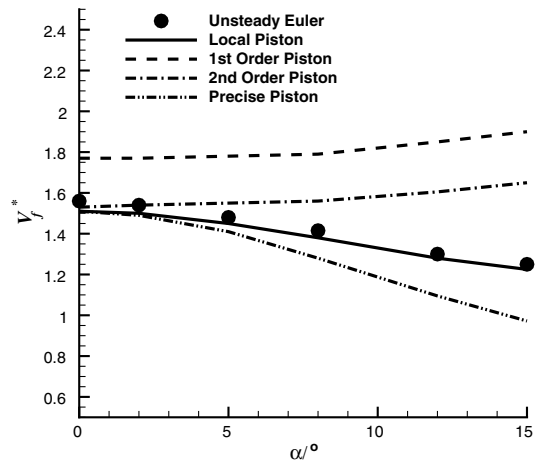

Fig. 13 Flutter speed vs angle of attack for the circular-arc airfoil at $M = 6$.
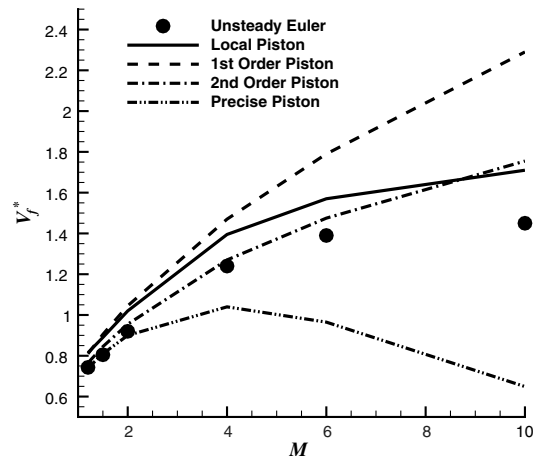

Fig. 14 Flutter speed vs M for the NACA64A010 airfoil at a 5 deg angle of attack.

Figure 14 compares the computed flutter speed of the NACA64A010 airfoil for different flight Mach numbers at a 5 deg fixed angle of attack. Figure 15 plots the results at the fixed flight Mach number $M = 6$, but for different angles of attack. Large errors exist of the classical piston theory results, except for low flight Mach numbers and at small angles of attack. Somewhat surprisingly, the second-order classical piston theory gives better results than the
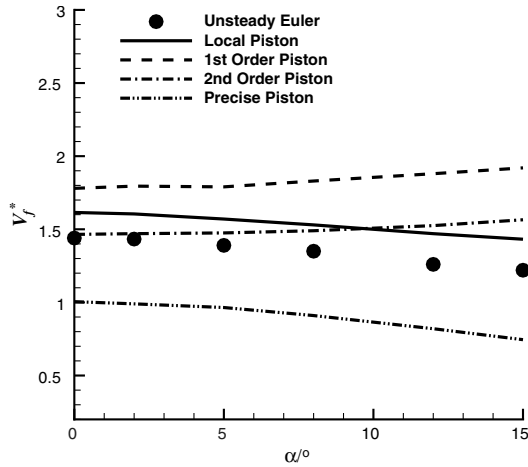

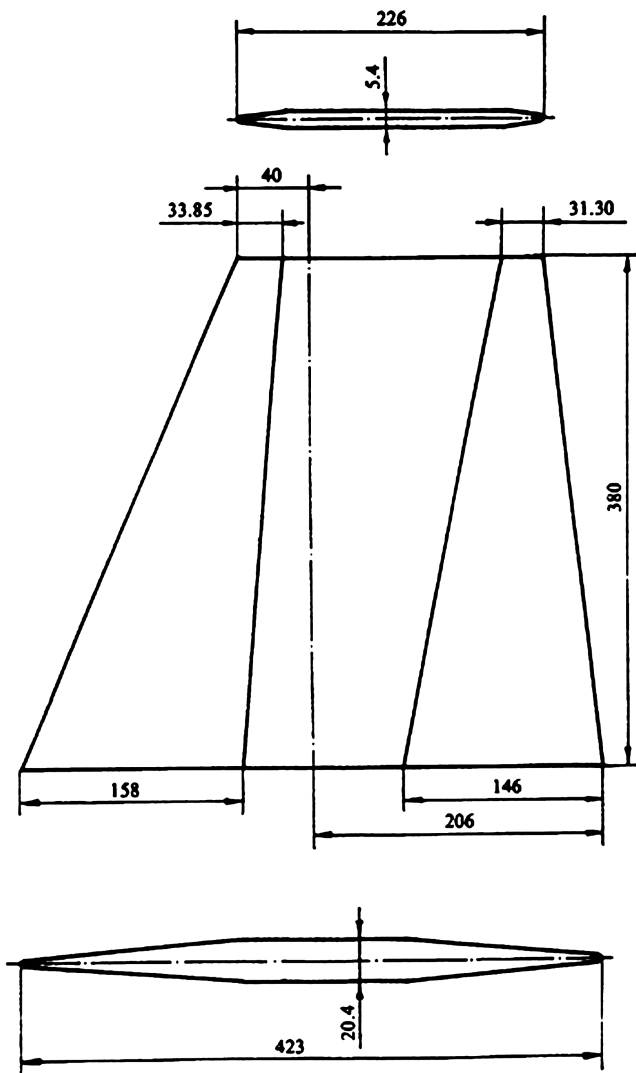Fig. 15 Flutter speed vs angle of attack for the NACA64A010 airfoil at $M = 6$.

Fig. 16 Shape of the rudder.

precise classical piston theory, but this is really a misleading paradox, because the classical theory simply is invalid for such an airfoil with a round leading edge because of the leading-edge singularity. The predictions by the local piston theory, although not as good as those for the circular-arc airfoil with a sharp leading edge, are arguably still within usable range.

B. Three-Dimensional Test Case

A trapeziform rudder with diamond airfoil section shown in Fig. 16 is used as a three-dimensional test case. Flutter experiments for this rudder were performed in [15] by tuning the structure to approach flutter at different flight conditions. To avoid uncertainties involved in the experiment and potential inaccuracy in the determination of the structural modes, we focus here on one fixed structure model. The first two mode shapes and modal frequencies of this model are shown in Fig. 17. The experimentally determined flutter speed is 606 m/s at Mach number 3.01 and 3.5 deg angle of attack with a freestream air density of 0.3362 kg/m^3. Figure 18 shows the time histories of the computed generalize coordinates of the coupled unsteady Euler simulations at the subcritical, critical, and super-critical flight speed at the given Mach number, angle of attack, and air density. Based on these simulations, the flutter speed is determined to be 618 m/s with the unsteady Euler method. Figure 19 depicts the root loci with the local piston theory method for this case, for which we determine 614 m/s as the flutter speed, which agrees with the predictions by the unsteady Euler method and is close to the experimental data.

We next increased the angle of attack with all other conditions fixed and performed the same computations. The predicted flutter speeds by the three methods are shown in Fig. 20. The classical piston theory in its full form agrees well with the local piston theory and the
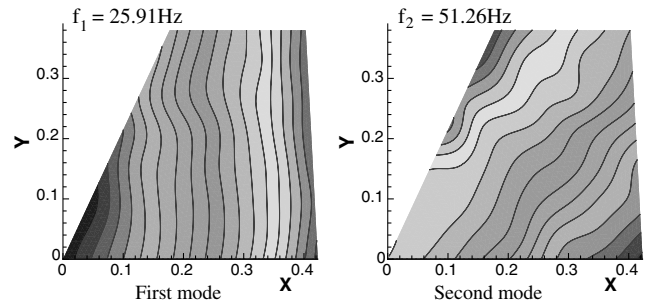

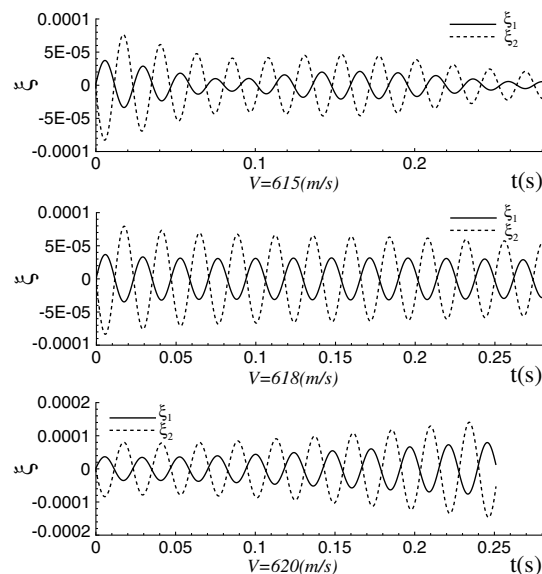Fig. 17 Mode shapes and modal frequencies for the rudder.

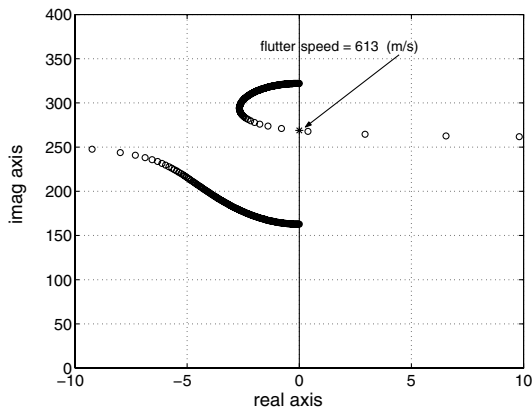Fig. 18 Responses of the ruder at different speeds by the unsteady Euler method at $\alpha = 3.5$ deg and $M = 3.01$.

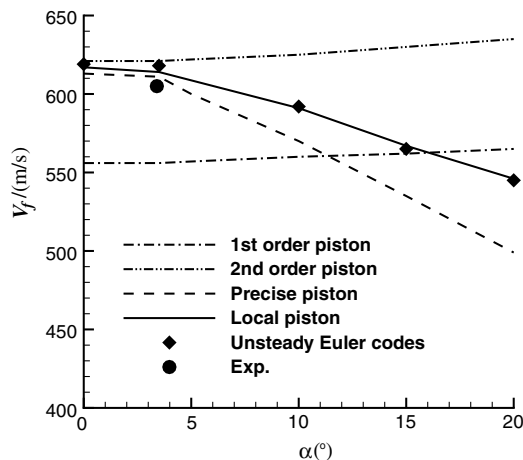**Fig. 19 Root loci by the local piston method at α = 3.5 deg and M = 3.01.**

Fig. 20 Flutter speeds of variation with angle of attack at M = 3.01.

full unsteady Euler method at low angles of attack. The errors of the classical piston theory increase significantly as the angles of attack increases beyond 5 deg, resulting in large underpredictions of the flutter speed. The local piston theory, on the other hand, almost goes through the predictions by the full unsteady Euler method in the full range of angle of attack up to 20 deg.

V. Conclusions

The classical piston theory is an extremely efficient method to calculate unsteady aerodynamic loads over slender wings with sharp leading edges at small angles of attack and not-too-low but also not-too-high supersonic speeds. Methods based on the unsteady Euler or Navier–Stokes equations remove those limitations but are computationally expensive and involve complexities in dealing with moving and deforming grids. We developed a highly efficient local piston theory for the prediction of inviscid unsteady pressure loads at supersonic and hypersonic speeds. Unlike the classical piston theory, this local piston theory separates the total air loads into a steady mean part caused by the mean location of the wing and that of unsteady fluctuations due to the motion of the wing around its mean location. The steady mean flow solution is first obtained by a full Euler method, which removes limitations on the airfoil thickness, angle of attack, flight Mach number, and leading-edge sharpness. The classical piston theory is then applied locally at each point on the airfoil surface on top of the mean steady flow to obtain the unsteady pressure perturbations caused by the relatively small deviation of the airfoil surface from its mean location. The resultant local piston theory is shown to have essentially removed the limitations of the classical piston theory on flight Mach number, airfoil thickness, and angles of attack for practical purposes. In addition, the method is also

demonstrated to yield reasonable accuracy for airfoils with round leading edges in a supersonic flow. Compared with the unsteady Euler method, which needs hundreds or even thousands of equivalent steady solutions with moving or deforming grids, the local piston theory requires only one steady-state solution without the use of moving or deforming grids. Its linear functional form of the unsteady pressure on the shape and velocity of the wing surface also makes it possible to perform flutter predictions by using the eigenvalue method with no need to perform time-domain coupled fluid–structure simulations.

References

[1] Gupta, K. K., and Voelker, L. S., "CFD-Based Aeroelastic Analysis of the X-43 Hypersonic Flight Vehicle," AIAA Paper 01-0712, 2001.
[2] Alonso, J. J., and Jameson, A., "Fully-Implicit Time-Marching Aeroelastic Solutions," AIAA Paper 94-0056, 1994.
[3] Liu, F., Cai, J., Zhu, Y., Tsai, H. M., and Wong, A. S. F., "Calculation of Wing Flutter by a Coupled Fluid-Structure Method," *Journal of Aircraft*, Vol. 38, No. 2, 2001, pp. 334–342.
doi:10.2514/2.2766
[4] Friedmann, P., McNamara, J. J., Thuruthimattam, B. J., and Nydick, I., "Aeroelastic Analysis of Hypersonic Vehicles," *Journal of Fluids and Structures*, Vol. 19, No. 5, 2004, pp. 681–712.
doi:10.1016/j.jfluidstructs.2004.04.003
[5] Lighthill, M. J., "Oscillating Airfoils at High Mach Number," *Journal of the Aeronautical Sciences*, Vol. 20, No. 6, 1953, pp. 402–406.
[6] Van Dyke, M. D., "Supersonic Flow Past Airfoils Including Nonlinear Thickness Effect," NACA 1183, 1953.
[7] Ashley, H., and Zartarian, G., "Piston Theory—A New Aerodynamic Tool for the Aeroelastician," *Journal of the Aeronautical Sciences*, Vol. 23, No. 12, 1956, pp. 1109–1118.
[8] Mei, C., Abdel-Motagaly, K., and Chen, R. R., "Review of Nonlinear Panel Flutter at Supersonic and Hypersonic speeds," *Applied Mechanics Reviews*, Vol. 52, No. 10, 1999, pp. 321–332.
doi:10.1115/1.3098919
[9] Liu, D. D., Yao, Z. X., Sarhaddi, D., and Chaves, F., "From Piston Theory to a Unified Hypersonic Supersonic Lifting Surface Method," *Journal of Aircraft*, Vol. 34, No. 3, 1997, pp. 304–312.
doi:10.2514/2.2199
[10] Liu, D. D., James, D. K., Chen, P. C., and Pototzky, A. S., "Further Studies of Harmonic Gradient Method for Supersonic Aeroelastic Applications," *Journal of Aircraft*, Vol. 28, No. 9, 1991, pp. 598–605.
doi:10.2514/3.46070
[11] Wang, G., "New Type of Grid Generation Technique together with the High Efficiency and High Accuracy Scheme Researches for Complex Flow Simulation," Ph.D. Dissertation, Northwestern Polytechnical Univ., Xi'an, China, 2005.
[12] Zhang, W., "Efficient Analysis for Aeroelasticity Based on Computational Fluid Dynamics," Ph.D. Dissertation, Northwestern Polytechnical Univ., Xi'an, China, 2006 (in Chinese).
[13] Zhang, W., and Ye, Z., "Two Better Loosely Coupled Solution Algorithms of CFD Based Aeroelastic Simulation," *Engineering Applications of Computational Fluid Mechanics*, Vol. 1, No. 4, 2007, pp. 253–262.
[14] Zhang, W., and Ye, Z., "Control Law Design for Transonic Aeroservo-elasticity," *Aerospace Science and Technology*, Vol. 11, Nos. 2–3, 2007, pp. 136–145.
doi:10.1016/j.ast.2006.12.004
[15] Bai, K., Feng, M., and Fu, G., "Flutter Experiment for Supersonic Rudder," *The Seventh Chinese Conference on Aeroelasticity*, Huzhou, Zhejiang, China, Oct. 2001, pp. 40–46 (in Chinese).

P. Beran
Associate Editor